CHIRALITY 19:716–730 (2007)

Application of Chiral Technology in a Pharmaceutical Company. Enantiomeric Separation and Spectroscopic Studies of Key Asymmetric Intermediates Using a Combination of Techniques. Phenylglycidols

OLIVER MCCONNELL,* YANAN HE, LISA NOGLE, AND ANI SARKAHIAN
Wyeth Research, Chemical and Screening Sciences, Collegeville, Pennsylvania

ABSTRACT Phenylglycidols substituted in the 2-, 3-, and 4- positions with fluorine, chlorine, and trifluoromethyl, and with methoxy in the 3- position, were synthesized from the corresponding *E*-cinnamic acids and separated into their (*R,R*)- and (*S,S*)- enantiomers using subcritical fluid chromatography with mixtures of MeOH in CO_2, on either a Chiralpak AD or AS chiral stationary phase. These compounds and commercially-available (*R,R*)- and (*S,S*)-phenylglycidol were analyzed for their vibrational circular dichroism (VCD), electronic circular dichroism (ECD), and optical rotation (OR) properties to exemplify a strategy whereby the absolute stereochemistry of common and key chiral intermediates is established early in the structure-activity and structure-property relationship phase of a drug discovery program in a pharmaceutical company. From this study, substituents in the phenyl group of the synthesized molecules were found not to grossly alter spectroscopic features, and therefore, diagnostic absorption bands in the respective VCD spectra, and the sign and shape of the measured ECD curves could be used to determine and track the absolute stereochemistry of analogs without necessarily requiring time-consuming *ab initio* calculations of all low energy conformers for all compounds. VCD, OR, and ECD calculations for the determination of absolute configuration carried out at the DFT level with the hybrid B3PW91 functional and the TZVP basis set were found to be especially useful in this study. *Chirality 19:716–730, 2007.*

KEY WORDS: supercritical fluid chromatography; chiral separations; enantiomeric separations; vibrational circular dichroism; electronic circular dichroism; optical rotation; determination of absolute stereochemistry; phenylglycidol

INTRODUCTION

The paradigm for modern drug discovery in many pharmaceutical companies involves taking several lead series from an Exploratory phase through a Discovery phase, and then selecting several compounds for Pre-Development. These compounds are typically designated as the lead, backup, and follow-on compounds. A lead series may involve a key chiral intermediate, which may be prepared through chiral starting materials, asymmetric synthesis, asymmetric enzymatic transformation, chiral salt resolution, or preparative enantiomeric separation.[1–11] Critical to understanding fully the structure-activity relationships (SAR)[12–14] and structure-property relationships (SPR)[15–19] often based on "pharmaceutical profiling"[20] is knowing the absolute stereochemistry of each analog prepared or separated, and being able to track the absolute stereochemistry to the final product with the desired biological activity profile (eutomer) and desirable drug-like properties, instead of the undesired profile (distomer).[21,22] Idealized steps in drug discovery can be summarized as follows:

- Target design;
- Design of synthesis and synthesis automation;
- Synthesis, including use of tools such as reaction blocks, microwave reactors, automated (achiral) prep HPLC, speed-vacuum evaporation, among others;
- Preparative enantiomeric separation (when asymmetric synthesis or other methods are not employed);
- Analytical characterization, including absolute stereochemistry determination;
- Sample submission to compound library;
- Biological evaluation of submitted compound (for SAR);
- Pharmaceutical profiling evaluation (for SPR);
- Results analysis (i.e., SAR and SPR);
- Redesign of target, and repeat cycle.

Much of the material in this manuscript was presented previously in a poster presentation at the ISCD-17/Chirality-2005, September 11–14, Parma, Italy.

Ani Sarkahian is currently at GSK, King of Prussia, PA.

*Correspondence to: Oliver J. McConnell, Discovery Analytical Chemistry, Chemical and Screening Sciences, Wyeth Research, 500 Arcola Road, Collegeville, PA 19426, USA. E-mail: mcconno@wyeth.com

Received for publication 18 August 2006; Accepted 17 November 2006
DOI: 10.1002/chir.20368
Published online 23 February 2007 in Wiley InterScience (www.interscience.wiley.com).

TABLE 1. Chiral technology tools in drug discovery

Analysis and preparation or purification of enantiomers:
(Automated) analytical and preparative HPLC
(Automated) analytical and preparative SFC
Determination of absolute stereochemistry:
X-ray crystallography
Circular dichroism (CD) (exciton chirality and porphyrin tweezers)
Measured versus calculated and comparison methods:
VCD
ECD
OR
NMR methods:
(Modified) Mosher's methods
Chiral liquid crystals

Based on the need to continually reassess and improve strategies, including shortening timelines for discovery projects, methodologies that speed up the process at any step represent important advances in drug discovery.

Excellent tools are available to the analytical chemist in modern drug discovery for preparative enantiomeric separation and analysis, and determination of absolute stereochemistry as seen in Table 1.

Currently, the tools used routinely in drug discovery for enantiomeric separations include analytical and preparative HPLC and sub- and supercritical SFC (subcritical fluid chromatography) that employ primarily polysaccharide, Pirkle-type and antibiotic chiral stationary phases (CSPs).[6–9,23–25] Analytical determination of enantiomeric excess can also be carried out when chiral starting materials, asymmetric synthesis, asymmetric enzymatic transformation, or chiral salt resolution are used for preparation of chiral intermediates and final products.

X-ray crystallography[26,27] is commonly viewed as the most reliable technique for the determination of absolute stereochemistry. However, the caveats for this approach are (1) the ability to prepare crystals suitable for analysis and (2) the recognition that X-ray analysis may be incorrect, albeit rarely.[28,29] NMR methods, including the Mosher's- or Trost-type approach is commonly used when functional groups such as secondary alcohols, primary amines or carboxylic acids are available for derivatization.[30,31] Comparison of specific optical rotation values and circular dichroism curves are used when a compound of known configuration is prepared.[32] Alternatively, when a compound expresses exciton coupling that is observed in the CD spectrum, the absolute stereochemistry can be assessed in combination with molecular modeling studies of the lowest energy conformers.[33–36] So-called porphyrin tweezers have also been used in combination with CD to determine absolute stereochemistry.[37–39] More recently, the spectroscopic approach of comparing observed and calculated vibrational circular dichroism (VCD) spectra, electronic circular dichroism (ECD), or optical rotation (OR) values has gained popularity due to the ease of data acquisition and the ability to calculate spectra and values with commercially available software and supercomputers or modern, powerful PCs and Linux clusters.[40–49] In the case of VCD, besides absolute stereochemistry of molecules containing one or more asymmetric centers, or planes or axes of asymmetry, i.e., atropisomerism,[50–53] additional information can be obtained, including solution conformation[54,55] and real-time reaction monitoring.[56,57] VCD has been applied specifically to pharmaceutically-relevant molecules.[58,59] Sometimes, however, difficulties may be encountered when applying one or more of these techniques, for example CD[60] or OR.[61]

(2*R*,3*R*)- and (2*S*,3*S*)-Phenylglycidol and substituted phenylglycidols represent rather simple molecules; however, they feature functionality that can yield chiral intermediates or final compounds with one or more asymmetric centers. Examples include fenfluramine, fluoxetine, taxol, and pseudoephedrine, among others (Fig. 1).[62–75]

These compounds display great versatility as common chiral intermediates, are easily prepared from readily available starting materials, and have low molecular weights combined with a limited number of conformers. As such, they were chosen as instructive examples to examine the effects on the chiroptical properties of these molecules with phenyl group substitution as calculated and measured by VCD, ECD, and OR. Therefore, in this study, 10 analogs were prepared as racemates, enantiomerically separated by SFC, and their absolute configurations determined by VCD and OR. Calculated electronic CD detection was also attempted. All of these results were compared with those obtained from commercially-available (2*R*,3*R*)- and (2*S*,3*S*)-phenylglycidol.

MATERIALS AND METHODS

The commercially-available chemicals, 2-, 3-, and 4-fluoro-, chloro- and trifluoromethylphenyl- and 3-methoxyphenyl-*E*-cinnamic acids, sodium borohydride, ethyl chloroformate, triethylamine, 3-chloroperoxybenzoic acid, and reaction solvents were purchased from Sigma-Aldrich (St. Louis, MO) and used as received. All HPLC, LC-MS, and SFC solvents were purchased from EM Science (aka/EMD Chemicals, Gibbstown, NJ), and formic acid used for LC-MS analysis was acquired from J.T. Baker (through VWR, West Chester, PA). The carbon dioxide used for SFC was purchased from Airgas East (Montgomeryville, PA; liquid carbon dioxide—industrial grade, 98% purity, 180 l/350 psi Dewars). It was further purified in situ using a Berger GDS-3000 Gas Delivery System to >99.9% purity (Mettler-Toledo AutoChem, Newark, DE). Medium pressure silica gel chromatography was carried out on an Isco Combi-Flash Sg 100c separation system equipped with UA-6 UV/Vis detector, Foxy Jr fraction collector, and PeakTrak software (Lincoln, NE). NMR data were recorded on a Varian AS400 spectrometer (^{1}H at 400 MHz) in $CDCl_3$. Chemical shifts are expressed in the δ scale and referenced to $CDCl_3$ (δ7.28). Coupling constants are given in Hz. Nominal mass–mass spectra were obtained from a Waters single-quadrupole LC/MS system that employs both positive and negative electrospray ionization on the Micromass ZQ mass spectrometer with the OpenLynx 4.0 software pack-

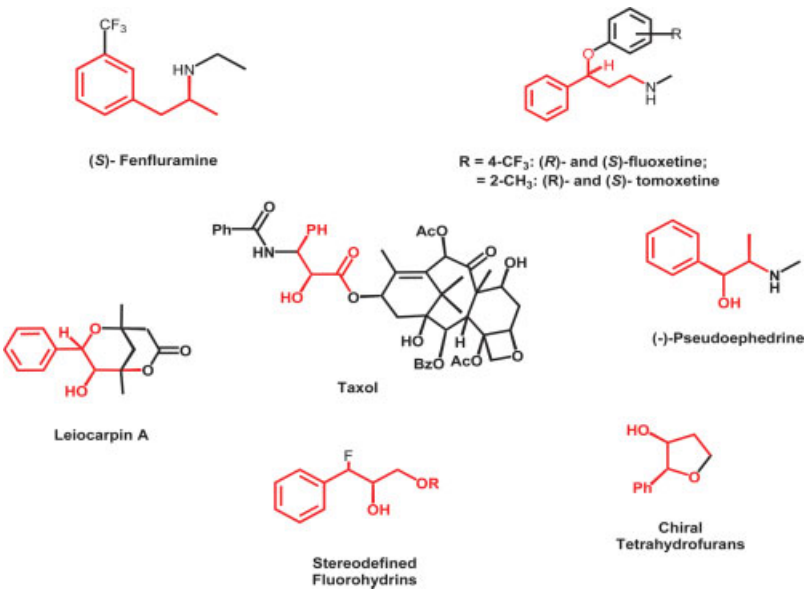

Fig. 1. Examples of compounds with one or more asymmetric centers that incorporate phenylglycidol, including fenfluramine, fluoxetine, taxol, pseudoephedrine, among others (phenylglycidol highlighted in red; see references in text).

age, a Waters Alliance 2695 HPLC unit, and Waters 996 photodiode array detector.

Preparation of Cinnamyl Alcohols[76]

The respective *E*-cinnamic acid (5 mmol) was dissolved in anhydrous THF (20 ml) and placed in a flask purged with N_2 and cooled to 0°C with an ice bath. Triethylamine (5 mmol) was then added. Ethyl chloroformate (5 mmol) in anhydrous THF (3 ml) was slowly added to the reaction mixture and stirred at 0°C for 0.5 h. The solution was filtered and the filtrate added directly to a solution of $NaBH_4$ (0.51 g) in water (7 ml) and the mixture stirred overnight at room temperature. The solution was acidified and worked up. The crude products were purified using medium pressure silica gel chromatography with 5% IPA in hexane. The yields were not optimized and, following chromatography, ranged from 40–54%. NMR and mass spectral data were consistent with the respective reaction products.

Preparation of Substituted Phenylglycidols[77]

The substituted *E*-cinnamyl alcohol (3 mmol) was dissolved in CH_2Cl_2 (25 ml) and 3-chloroperoxybenzoic acid (3 mmol) was then added. The reaction mixture was stirred overnight at room temperature. The organic layer was worked up in the usual manner. The crude products were purified using medium pressure silica gel chromatography with 5% IPA in hexane. The yields were not optimized and, following chromatography, ranged from 38%–86%.

***rac* 2-Chlorophenylglycidol (2).** Colorless oil, 66% isolated yield. Mass Spec: $[M+H]^+ = 184.1$. NMR: 7.31 (m, 1H), 7.21 (m, 3H), 4.22 (d, $J = 2$, 1H), 4.05 (dd, $J = 2$, and 13, 1H), 3.82 (d, $J = 2$, and 13, 1H), 3.06 (m, 1H), 1.76 (br s, 1H).

***rac* 2-Fluorophenylglycido (3).** Colorless oil, 50% isolated yield. Mass Spec: $[M+H]^+ = 168.2$. NMR: 7.24 (m, 1H), 7.17 (m, 1H), 7.09 (m, 1H), 7.01 (m, 1H), 4.17 (d, $J = 2$, 1H), 4.03 (dd, $J = 2$, and 13, 1H), 3.78 (dd, $J = 4$, and 13, 1H), 3.19 (m, 1H), 1.77 (br s, 1H).

***rac* 2-Trifluoromethylphenylglycidol (4).**[78] White solid, 55% isolated yield. Mass Spec: $[M+H]^+ = 218.2$. NMR: 7.39–7.66 (m, 4H), 4.25 (s, 1H), 4.06 (m, 1H), 3.81 (M, 1H), 3.06 (m, 1H), 1.67 (m, 1H).

***rac* 3-Chlorophenylglycidol (5).**[78] Colorless oil, 55% isolated yield. Mass Spec: $[M+H]^+ = 184.2$. NMR: 7.22–7.25 (m, 3H), 7.14 (m, 1H), 4.02 (d, $J = 13$, 1H), 3.88 (d, $J = 2$, 1H), 3.78 (d, $J = 13$, 1H), 3.14 (m, 1H), 1.74 (br s, 1H).

***rac* 3-Fluorophenylglycidol (6).**[79] Colorless oil, 64% isolated yield. Mass Spec: $[M+H]^+ = 168.2$. NMR: 7.26 (m, 1H), 7.05 (d, $J = 8$, 1H), 6.93–6.99 (m, 2H), 4.01 (dd, $J = 2$, and 13, 2H), 3.90 (d, $J = 2$, 1H), 3.78 (dd, $J = 4$, and 13, 1H), 3.14 (m, 1H), 1.75 (br s, 1H).

***rac* 3-Methoxyphenylglycidol (7).**[80] Colorless oil, 35% isolated yield. Mass Spec: $[M+H]^+ = 180.2$. NMR: 7.23 (m, 1H), 6.77–6.86 (m, 3H), 4.01 (d, $J = 13$, 1H), 3.88 (d, $J = 2$, 1H), 3.79 (s, 1H), 3.77 (s, 3H), 3.17 (m, 1H), 1.76 (br s, 1H).

***rac* 3-Trifluoromethylphenylglycidol (8).**[81] Colorless oil, 38% isolated yield. Mass Spec: $[M+H]^+ = 218.2$. 7.46–7.55 (m, 2H), 7.22–7.45 (m, 2H), 4.03 (dd, $J = 2$, and 13, 1H), 3.97 (d, $J = 2$, 1H), 3.80 (d, $J = 12$, 1H), 3.17 (m, 1H), 1.72 (br s, 1H).

***rac* 4-Chlorophenylglycidol (9).**[82] Colorless oil, 68% isolated yield. Mass Spec: $[M+H]^+ = 184.1$. NMR: 7.31–7.34 (m, 2H), 7.20–7.26 (m, 2H), 4.05 (d, $J = 13$, 1H), 3.92 (d, $J = 2$, 1H), 3.78–3.84 (m, 1H), 3.18 (m, 1H), 1.82 (br s, 1H).

***rac* 4-Fluorophenylglycidol (10).**[82] Colorless oil, 86% isolated yield. Mass Spec: $[M+H]^+ = 168.2$. NMR: 7.19–7.24 (m, 2H), 6.97–7.05 (m, 2H), 4.01 (d, $J = 13$, 1H), 3.88 (d, $J = 2$, 1H), 3.78 (d, $J = 12$, 1H), 3.15 (m, 1H), 1.77 (br s, 1H).

***rac* 4-Trifluoromethylphenylglycidol (11).**[82] White solid, 54% isolated yield. Mass Spec: $[M+H]^+ = 218.2$. NMR: 7.61 (d, $J = 8$, 2H), 7.41 (d, $J = 8$, 2H), 4.08 (d, $J = 13$, 1H), 4.01 (d, $J = 2$, 1H), 3.85 (d, $J = 13$, 1H), 3.19 (m, 1H), 1.78 (br s, 1H).

The enantiomers of the aforementioned compounds showed identical NMR and LC-MS data: All (2R,3R) enantiomers will be defined as **a** and the (2*S*,3*S*) as **b**.

Analytical Enantiomeric HPLC of the Substituted Phenylglycidols[83]

This was performed on an Agilent 1100 system (Agilent Technologies, Inc) using the CSP, Chiralpak AD-H (tris-3,5-dimethylphenylcarbamate; 4.6 × 250 mm, 5 μm), which was purchased from Chiral Technologies (Exton, PA). Flow: 1.0 mL/min, 35% EtOH/65% Hexane, UV at 225 nm. All enantiomers, chirally purified from preparative SFC, possessed >95% enantiomeric excess with the following exceptions: (*2R*,3*R*)-4-fluorophenylglycidol (**10a**, 82.6% *ee*), (*2R*,3*R*)-4-chlorophenylglycidol (**9a**, 85.0% *ee*), and (*2S*,3*S*)-4-fluorophenylglycidol (**10b**, 94.1% *ee*).

Preparative Enantiomeric Separation

The racemic phenylglycidols were enantiomerically separated using the Berger SFC Multigram I stacked-injection supercritical fluid chromatographic (SFC) system (Mettler-Toledo AutoChem) with the Chiralpak AD-H and AS-H CSPs (20 mm id × 25 cm length, 5 μm) (Chiral Technologies) using MeOH in CO_2. VCD, ECD, and OR data of the isolated enantiomers are shown later.

VCD Measurements

VCD and IR spectra were measured using a Chiral*ir* spectrophotometer modified with dual-PEMS[40] (Biotools, Wauconda, IL). In the absorption spectra presented, the solvent absorption was removed by subtraction. Each enantiomer was dissolved in $CDCl_3$ at a concentration of 5–10 mg/100 μl and measured in a BaF cell (path length, 100 μm). Acquisition times were 4 h using 1-h time blocks with 4 cm^{-1} resolution (PEM set at 1400 cm^{-1}). (The VCD baselines were obtained by subtracting the VCD of one enantiomer from the other and then dividing by two.)

ECD Measurements

Electronic CD spectra were measured with a JASCO J-715 spectropolarimeter (Jasco, Easton, MD). Spectra were acquired in MeOH (~15 mM) in a quartz cell with a 1 cm path length.

OR Measurements

ORs were measured at room temperature (23°C) with a JASCO P-1020 polarimeter (Jasco). The concentrations of the samples were ~10 mg/ml ($c = 1$ (1 g/100 ml)). The values shown below are at the concentrations given and not those obtained by extrapolation to zero concentration as recommended by Polavarapu et al.[43]

VCD, ECD and OR Calculation Protocol

Conformers of the substituted phenylglycidols were built using HyperChem 7.0 (Hypercube, Gainesville, FL) and optimized using the PM3 semi-empirical method. Prediction of the unpolarized absorption (IR) and VCD intensities and frequencies, electronic CD intensities and frequencies, and OR at 589 nm spectra of the lowest energy conformers were carried out using Gaussian 03 at the DFT level with the B3LYP/6-31G(d) and B3PW91/TZVP hybrid functionals and basis sets utilizing the magnetic field perturbation method with gauge invariant atomic orbitals (Gaussian, Wallingford, CT). To compare calculated VCD spectra with experimental spectra, computed frequencies were uniformly scaled by a factor of 0.97 and the intensities were converted to Lorentzian bands with a 6 cm^{-1} half-width at half-height for presentation as Axum 6 plots (Mathsoft, Cambridge, MA). The Boltzmann-population-weighted average of multiple conformers was calculated if the energy differences were within 1 Kcal/mol.

RESULTS AND DISCUSSION

The reduction and epoxidation reactions from the *E*-cinnamic acids substituted with fluorine, chlorine, trifluoromethyl, and methoxy groups proceeded smoothly (Scheme 1); yields were not optimized. The analogs, 2-methoxyphenylglycidol and 4-methoxyphenylglycidol, were not pursued in this study as, in our hands, these compounds were not stable; only the enantiomers of 3-methoxyphenylglycidol (**7a** and **7b**) were included in this study.

Preparative enantiomeric separation with stacked-injections of the respective racemic phenylglycidols was accomplished using mixtures of MeOH in hexane on the polysaccharide CSPs, Chiralpak AD-H, or AS-H. (e.g., chromatogram found in Fig. 2 for *rac* 4-trifluoromethylphenylglycidol (**11**)).

Ab initio calculation of the lowest energy *trans*-epoxide conformers of the (2*R*,3*R*)-enantiomers revealed the following: Phenylglycidol (**1a**) expressed one major low energy conformer (Fig. 3). 2-(**2a**) and 4-chloro-(**9a**), and 2-(**3a**) and 4-fluorophenylglycidol (**10a**) also featured only one low energy conformer (Fig. 3). Calculation of 3-chloro-(**5a**), and 2-(**4a**), 3-(**8a**), and 4-trifluoromethylphenylglycidol (**11a**) revealed two low energy conformers (C1 and C2, Fig. 4). Analysis of 3-fluorophenylglycidol (**6a**) provided three low energy conformers (C1, C2, and C3), and 3-methoxyphenylglycidol (**7a**) featured four low energy conformers (C1, C2, C3, and C4; Fig. 5). With the exception of (2*R*,3*R*)-2-trifluoromethylphenylglycidol (**4a**) (Fig. 4), the lowest energy conformer in all other compounds consisted of or included a C1–C2 gauche configuration

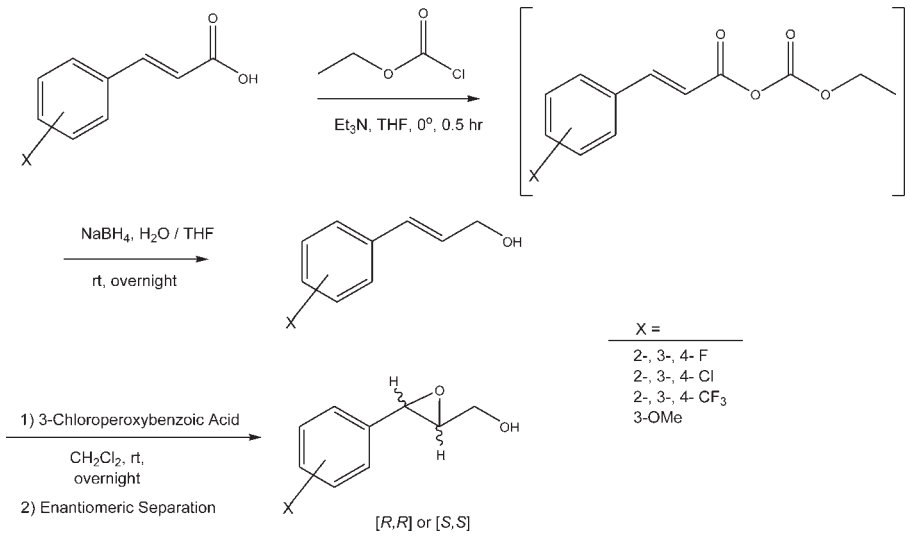

Scheme 1. Generalized reaction scheme of *rac*-phenylglycidol synthesis from *E*-cinnamic acids with substitution in the phenyl ring, followed by preparative enantiomeric separation.

whereby the oxygen on the primary hydroxyl moiety nearly bisects the C2 oxygen–C3 carbon bond of the oxirane ring, and the proton on the hydroxyl moiety is positioned to hydrogen-bond with the oxirane oxygen (Fig. 6a). An additional low energy conformer is found in (2*R*,3*R*)-3-fluorophenylglycidol (**6a**) (Fig. 5), where the alternate C1–C2 gauche configuration is observed, and again the proton on the hydroxyl moiety is positioned to hydrogen-bond with the oxirane oxygen (Fig. 6b). A third conformer is found in (2*R*,3*R*)-2-trifluoromethylglycidol (**4a**) (Fig. 4) where the oxirane oxygen is anti- to the hydroxyl moiety, and the hydroxyl proton is positioned to hydrogen-bond with the fluorines in the *ortho*-trifluoromethyl moiety (Fig. 6c). In those cases where the phenyl substituent is in the 2- or 3- position, where there is an element of asymmetry in the phenyl group, the phenyl rings can exhibit two stable conformations, interconverted by $\sim 180^{\circ}$ rotation around the C3–C4 bond.[84] In the cases of the 2-chloro-(**2a**), 2-fluoro-(**3a**), and 2-trifluoromethyl-(**4a**) substituents, the lowest energy conformers consist of those with the substituents effectively anti- with respect to the phenyl ring and the oxirane oxygen, presumably due to greater electrostatic repulsion of the substituents and the oxirane oxygen when co-located on the same face of the phenyl

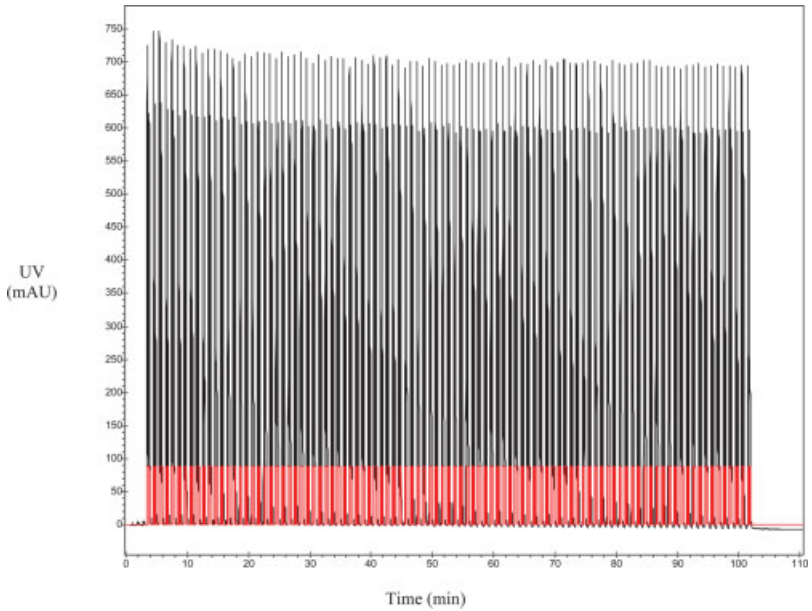

Fig. 2. Preparative enantiomeric separation of *rac*-4-trifluoromethylphenylglycidol using SFC with stacked injection on the Chiralpak AS (2 × 25 cm) CSP, 10% MeOH/90% CO_2, 50 ml/min flow rate, 220 nm UV detection, 100 bar outlet pressure, 20 mg/injection every 1.5 min.

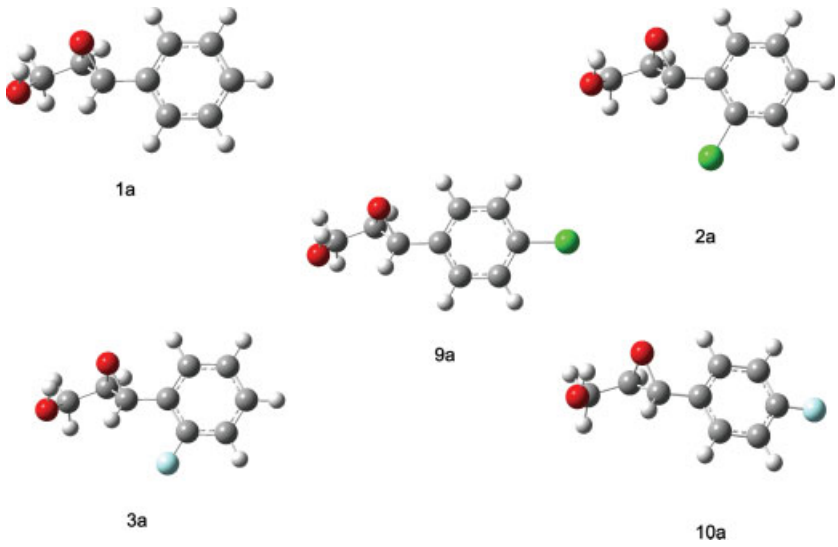

Fig. 3. Lowest energy conformer of (2*R*,3*R*)-phenylglycidol (**1a**), (2*R*,3*R*)-2-chlorophenylglycidol (**2a**), (2*R*,3*R*)-2-fluorophenylglycidol (**3a**), (2*R*,3*R*)-4-chlorophenylglycidol (**9a**), and (2*R*,3*R*)-4-fluorophenylglycidol (**10a**).

ring. And, as suggested earlier for the case of **4a**, possible hydrogen bonding between the hydroxyl proton and the *ortho*-trifluoromethyl fluorines may be the driving force for one of the low energy conformers that results in the substituents located anti- with respect to the oxirane oxygen. In contrast, the enantiomers with substituents in the 3-position, i.e., 3-chloro-(**5a**), 3-fluoro-(**6a**), 3-methoxy-(**7a**), and 3-trifluoromethyl-(**8a**) do not express a statistical preference regarding their orientation relative to the oxirane ring.

Calculated absorption and VCD of the low energy conformers of the analogs of (2*R*,3*R*)-phenylglycidol enantiomers at the DFT level with the B3LYP/6-31G(d) and B3PW91/TZVP functionals and basis sets with subsequent summing of the spectra using the Boltzmann distribution where multiple low energy conformers existed revealed a close match with the observed spectra of one of the enantiomers for each pair of the respective phenyl-substituted compounds. Although slight differences were observed between the DFT functionals and basis sets, a distinct advantage was not observed with either combination. Figure 7 provides a comparison of observed versus calculated absorption spectra for (2*R*,3*R*)-phenylglycidol (**1a**) and (2*R*,3*R*)-2-chloro- (**2a**), (2*R*,3*R*)-2-fluoro- (**3a**) and

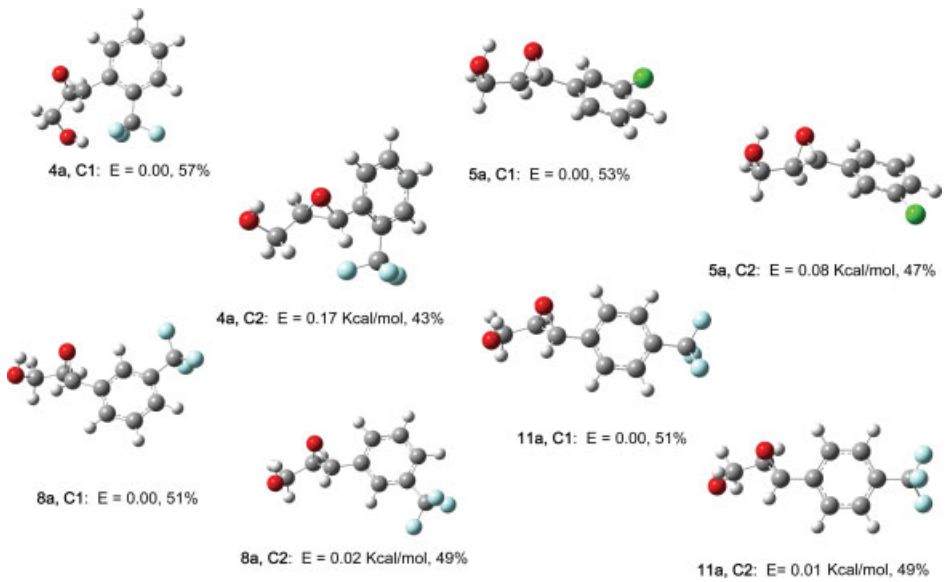

Fig. 4. Lowest energy conformers of (2*R*,3*R*)-2-trifluoromethylphenylglycidol (**4a**), (2*R*,3*R*)-3-chlorophenylglycidol (**5a**), (2*R*,3*R*)-3-trifluoromethylphenylglycidol (**8a**), and (2*R*,3*R*)-4-trifluoromethylphenylglycidol (**11a**), which feature two conformers that are within 1 kcal/mol; their relative energies (in Kcal/mol) and respective % population based on Boltzmann distribution are also shown.

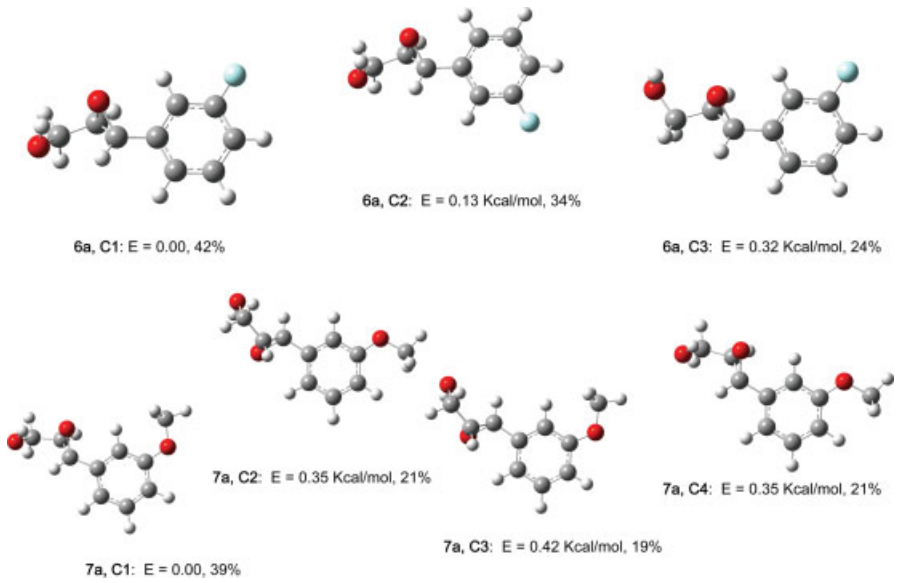

Fig. 5. Lowest energy conformers of (*2R*,*3R*)-3-fluorophenylglycidol (**6a**), and (*2R*,*3R*)-3-methoxyphenylglycidol (**7a**), which feature three conformers for **6a** and four conformers for **7a** that are within 1 Kcal/mol; their relative energies (in Kcal/mol) and respective % population based on Boltzmann distribution are also shown.

(*2R*,*3R*)-2-trifluoromethylphenylglycidol (**4a**); Figure 8 provides a comparison of observed versus calculated VCD spectra for (*2R*,*3R*)-phenylglycidol (**1a**) and (*2R*,*3R*)-2-chloro- (**2a**), (*2R*,*3R*)-2-fluoro- (**3a**), and (*2R*,*3R*)-2-trifluoromethylphenylglycidol (**4a**); Figure 9 provides a comparison of observed versus calculated absorption spectra for (*2R*,*3R*)-phenylglycidol (**1a**) and (*2R*,*3R*)-3-chloro- (**5a**), (*2R*,*3R*)-3-fluoro- (**6a**), (*2R*,*3R*)-3-methoxy- (**7a**), and (*2R*, *3R*)-3-trifluoromethylphenylglycidol (**8a**); Figure 10 provides a comparison of observed versus calculated VCD spectra for (*2R*,*3R*)-phenylglycidol (**1a**) and (*2R*,*3R*)-3-chloro- (**5a**), (*2R*,*3R*)-3-fluoro- (**6a**), (*2R*,*3R*)-3-methoxy- (**7a**), and (*2R*,*3R*)-3-trifluoromethylphenylglycidol (**8a**); Figure 11 provides a comparison of observed versus calculated absorption spectra for (*2R*,*3R*)-phenylglycidol (**1a**) and (*2R*,*3R*)-4-chloro- (**9a**), (*2R*,*3R*)-4-fluoro- (**10a**), and (*2R*,*3R*)-4-trifluoromethylphenylglycidol (**11a**); Figure 12 provides a comparison of observed versus calculated VCD spectra for (*2R*,*3R*)-phenylglycidol (**1a**) and (*2R*,*3R*)-4-chloro- (**9a**), (*2R*,*3R*)-4-fluoro- (**10a**), and (*2R*,*3R*)-4-trifluoromethylphenylglycidol (**11a**).

Subsequent DFT level calculation of the ORs at 589 nm for the (*2R*,*3R*) enantiomers followed by summing of the OR values using the Boltzmann distribution, where multiple low energy conformers existed showed that these enantiomers generally expressed positive rotations with the exceptions of (*2R*,*3R*)-2-chlorophenylglycidol (**2a**) and (*2R*,*3R*)-2-trifluoromethylphenylglycidol (**4a**), which were

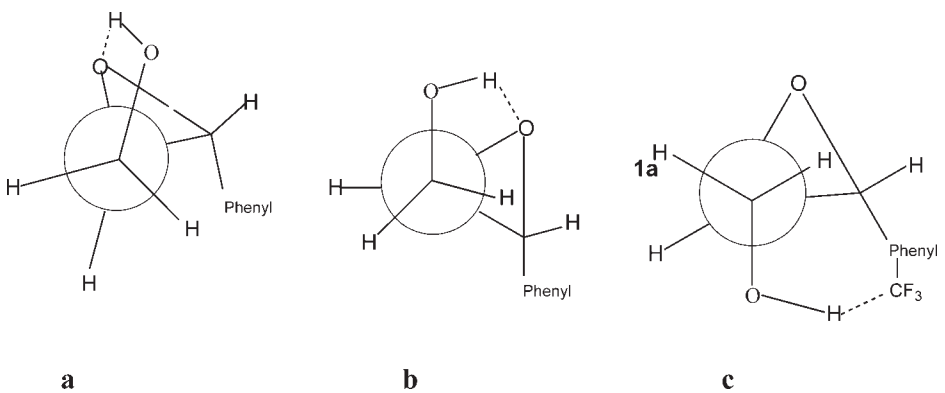

Fig. 6. (a) Newman projection of the lowest energy conformer in nearly all compounds with the exception of 2-fluorophenylglycidol (**4**) that included a C1−C2 gauche configuration whereby the oxygen on the primary hydroxyl moiety nearly bisects the oxygen −C3 carbon bond of the oxirane ring, and the proton on the hydroxyl moiety is positioned for hydrogen-bonding to the oxirane-oxygen, (b) alternate C1−C2 gauche configuration found in (*2R*,*3R*)-2-trifluoromethylglycidol (**4a, C2**) and (*2R*,*3R*)-3-fluorophenylglycidol (**6a, C3**), and (c) third conformer found in (*2R*,*3R*)-2-trifluoromethylglycidol (**4a, C1**) where the oxirane-oxygen is *anti*- to the hydroxyl moiety, and the hydroxyl proton is positioned for hydrogen-bonding to the fluorines in the *ortho*-trifluoromethyl moiety.

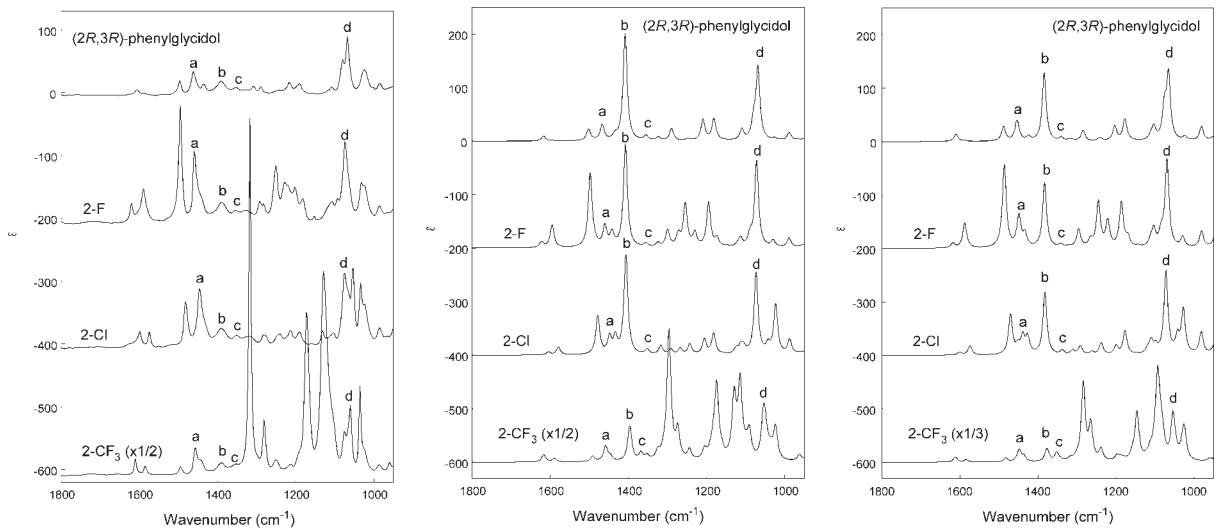

Fig. 7. Observed (left frame) and calculated (center and right frames) IR spectra of (2*R*,3*R*)-phenylglycidol (**1a**), (*2R*,3*R*)-2-chlorophenylglycidol (**2a**), (*2R*,3*R*)-2-fluorophenylglycidol (**3a**), and (*2R*,3*R*)-2-trifluoromethylphenylglycidol (**4a**). Samples (in $CDCl_3$) were measured in a 0.1 mm-path length BaF_2 cell with 4 cm^{-1} resolution, 4 h accumulation, and PEM optimized at 1400 cm^{-1}. Spectral baselines were obtained by subtracting the spectra of $CDCl_3$ from the sample spectra. Calculations were carried out with Gaussian03 at DFT level with B3LYP functional/6-31G(d) basis set (center frame) and with B3PW91 functional/TZVP basis set (right frame). Spectra are offset for clarity.

negative (Table 2). Comparing ORs alone in this series and assuming that all (2*R*,3*R*)- analogs feature positive rotations could be misleading.

As the specific rotations are generally large in this series, the comparison between measured values and calculation using the B3PW91/TZVP hybrid functional and basis set for the (2*R*,3*R*) enantiomers are sufficiently close to make unambiguous assignments. With the B3LYP/6-31G(d) functional and basis set, major discrepancies were found for (*2R*,3*R*)-2-trifluoromethylphenylglycidol (**4a**) and (*2R*,3*R*)-4-trifluoromethylphenylglycidol (**11a**), where the calculated values were effectively zero while the observed specific rotations are −15 and +27, respectively. Another major discrepancy was found for (*2R*,3*R*)-2-chlorophenylglycidol (**2a**), where the measured specific rotation was negative, −6 versus a positive calculated

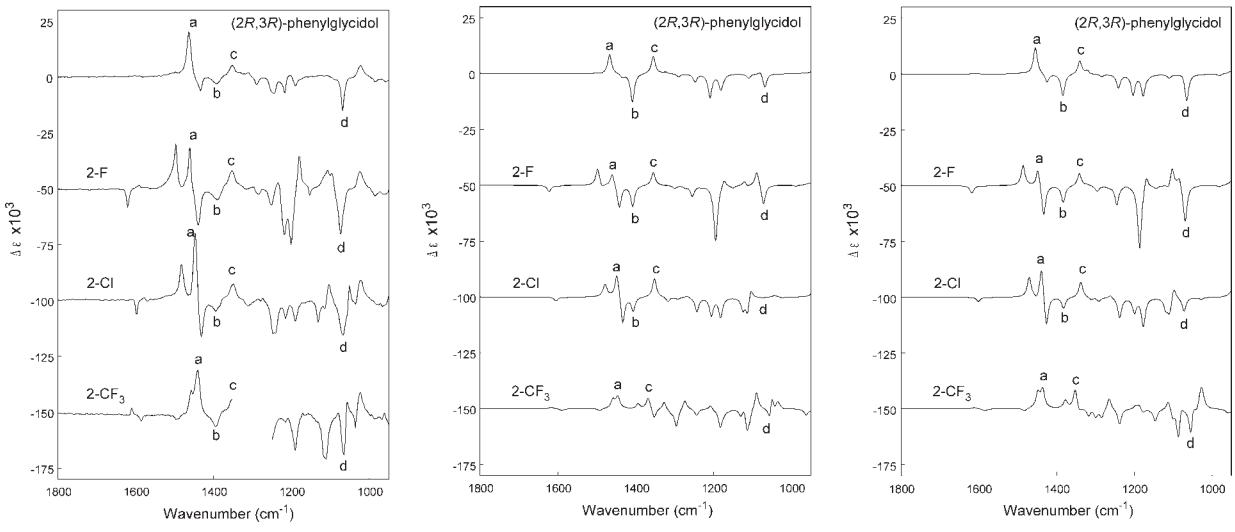

Fig. 8. Observed (left frame) and calculated (center and right frames) VCD spectra of (2*R*,3*R*)-phenylglycidol (**1a**), (*2R*,3*R*)-2-chlorophenylglycidol (**2a**), (*2R*,3*R*)-2-fluorophenylglycidol (**3a**), and (*2R*,3*R*)-2-trifluoromethylphenylglycidol (**4a**). Samples (in $CDCl_3$) were measured in a 0.1 mm-path length BaF_2 cell with 4 cm^{-1} resolution, 4 h accumulation, and PEM optimized at 1400 cm^{-1}. Spectral baselines were obtained by subtracting the spectra of $CDCl_3$ from the sample spectra. Calculations were carried out with Gaussian03 at DFT level with B3LYP functional/6-31G(d) basis set (center frame) and with B3PW91 functional/TZVP basis set (right frame). Spectra are offset for clarity.

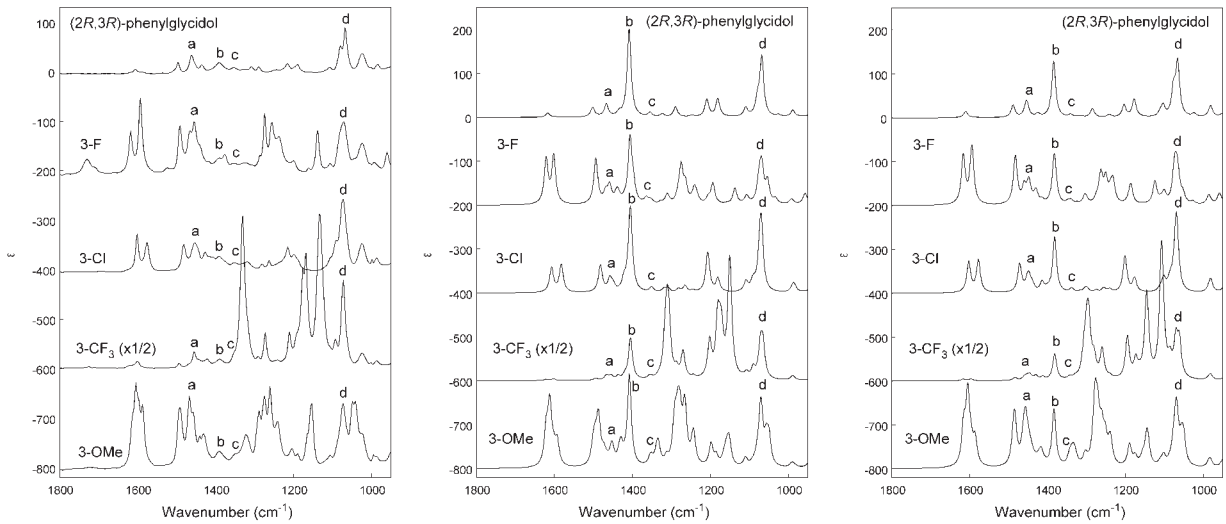

Fig. 9. Observed (left frame) and calculated (center and right frames) IR spectra of (2*R*,3*R*)-phenylglycidol (**1a**), (2*R*,3*R*)-3-chlorophenylglycidol (**5a**), (2*R*,3*R*)-3-fluorophenylglycidol (**6a**), (2*R*,3*R*)-3-methoxyphenylglycidol (**7a**), and (2*R*,3*R*)-3-trifluoromethylphenylglycidol (**8a**). Samples (in $CDCl_3$) were measured in a 0.1 mm-path length BaF_2 cell with 4cm^{-1} resolution, 4 h accumulation, and PEM optimized at 1400 cm^{-1}. Spectral baselines were obtained by subtracting the spectra of $CDCl_3$ from the sample spectra. Calculations were carried out with Gaussian03 at DFT level with B3LYP functional/6-31G(d) basis set (center frame) and with B3PW91 functional/TZVP basis set (right frame). Spectra are offset for clarity.

value of +108. In contrast to comparison between the observed and calculated VCD using the different DFT functionals and basis sets, the OR could be calculated with confidence using only the B3PW91/TZVP functional and basis set.

In the measured CD spectra, the samples expressing the (2*R*,3*R*) configuration by VCD and OR featured a significant λ_{min} at ~215–222 nm and a slight λ_{max} at ~224–235 nm (Fig. 13). DFT calculation using the B3PW91/TZVP functional and basis set generally provided a match with the observed values, and were consistent with the results found by comparing observed and measured VCD and OR. However, DFT level calculation of the ECD using the B3LYP/6-31G(d) functional and basis set did not compare especially well with the measured values (Table 3). In many of these cases, the calculated λ_{min} and λ_{max} were significantly shifted relative to the observed spectra, or these values were inverted.

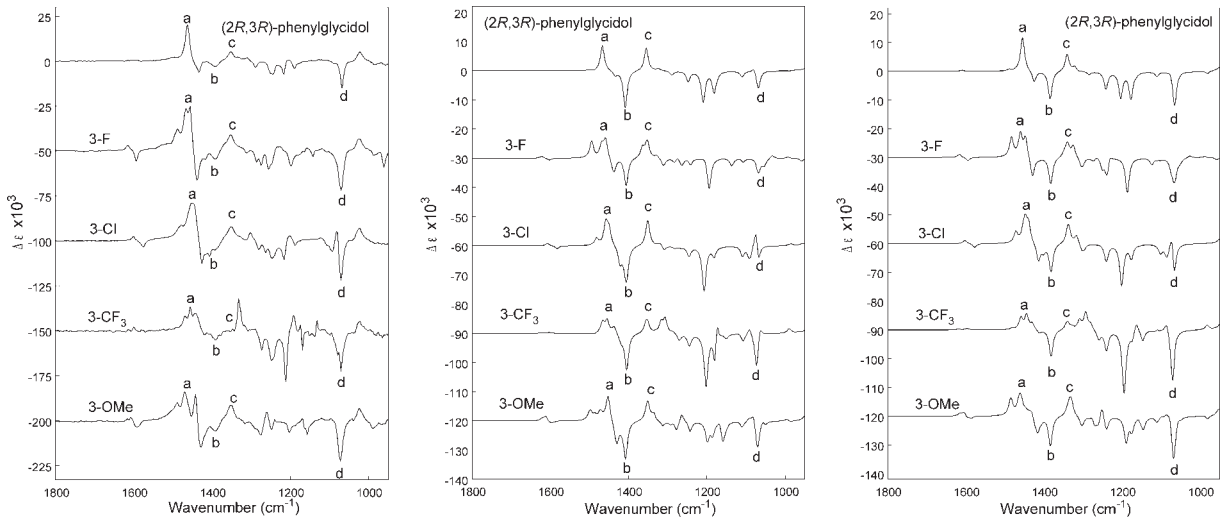

Fig. 10. Observed (left frame) and calculated (center and right frames) VCD spectra of (2*R*,3*R*)-phenylglycidol (**1a**), (2*R*,3*R*)-3-chlorophenylglycidol (**5a**), (2*R*,3*R*)-3-fluorophenylglycidol (**6a**), (2*R*,3*R*)-3-methoxyphenylglycidol (**7a**), and (2*R*,3*R*)-3-trifluoromethylphenylglycidol (**8a**). Samples (in $CDCl_3$) were measured in a 0.1 mm-path length BaF_2 cell with 4 cm^{-1} resolution, 4 h accumulation, and PEM optimized at 1400 cm^{-1}. Spectral baselines were obtained by subtracting the spectra of $CDCl_3$ from the sample spectra. Calculations were carried out with Gaussian03 at DFT level with B3LYP functional/6-31G(d) basis set (center frame) and with B3PW91 functional/TZVP basis set (right frame). Spectra are offset for clarity.

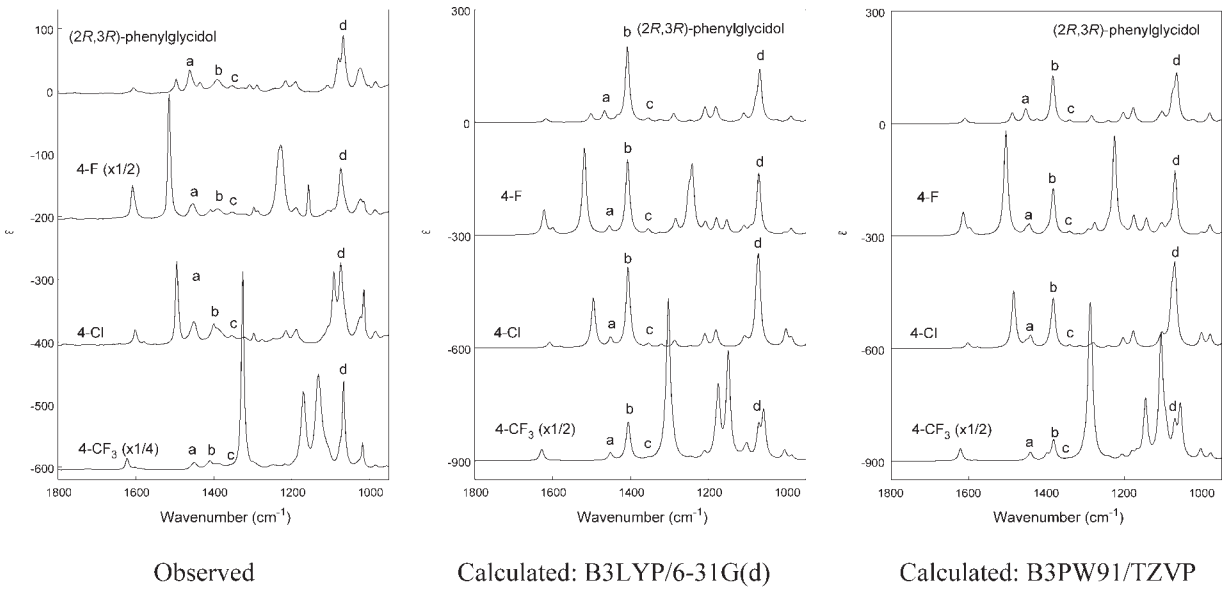

Fig. 11. Observed (left frame) and calculated (center and right frames) IR spectra of (2*R*,3*R*)-phenylglycidol (**1a**), (2*R*,3*R*)-4-Chlorophenylglycidol (**9a**), (2*R*,3*R*)-4-Fluorophenylglycidol (**10a**), and (2*R*,3*R*)-4-Trifluoromethylphenylglycidol (**11a**). Samples (in $CDCl_3$) were measured in a 0.1 mm-path length BaF_2 cell with 4 cm^{-1} resolution, 4 h accumulation, and PEM optimized at 1400 cm^{-1}. Spectral baselines were obtained by subtracting the spectra of $CDCl_3$ from the sample spectra. Calculations were carried out with Gaussian03 at DFT level with B3LYP functional/6-31G(d) basis set (center frame) and with B3PW91 functional/TZVP basis set (right frame). Spectra are offset for clarity.

Preparative SFC as well as chiral analysis of the enantiomers using Chiralpak AD or AS CSP revealed that the 2- and 3-substituted (2*S*,3*S*)- enantiomers typically eluted first, whereas the 4-substituted (2*R*,3*R*)- enantiomers eluted first in all cases (Table 4). Exceptions were found with (*2R*,3*R*)-2-trifluoromethylphenylglycidol (**4a**), (*2S*,3*S*)-2-trifluoromethylphenylglycidol (**4b**), (*2R*,3*R*)-3-methoxyphenylglycidol (**7a**), and (*2S*,3*S*)-3-methoxyphenylglycidol (**7b**), where **4a** and **7b** eluted first in HPLC and **4b** and **7a** eluted first in semipreparative SFC. In the case of **4a** and **4b**, Chiralpak AD-H was used for both analytical HPLC and preparative SFC separations, whereas in the

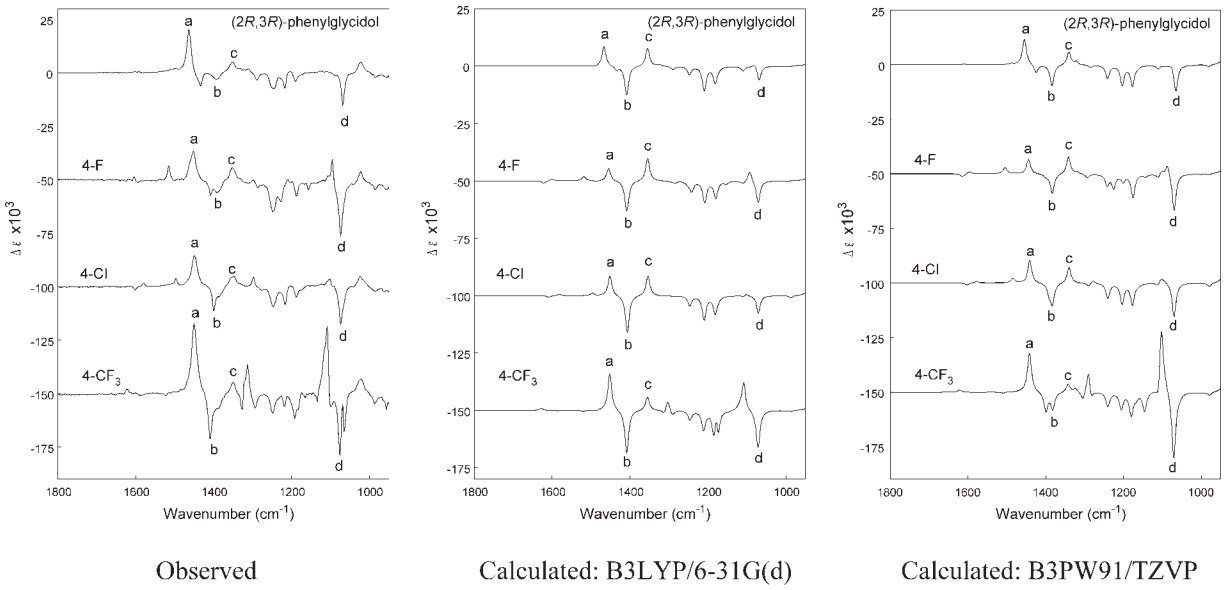

Fig. 12. Observed (left frame) and calculated (center and right frames) VCD spectra of (2*R*,3*R*)-phenylglycidol (**1a**), (2*R*,3*R*)-4-Chlorophenylglycidol (**9a**), (2*R*,3*R*)-4-Fluorophenylglycidol (**10a**), and (2*R*,3*R*)-4-Trifluoromethylphenylglycidol (**11a**). Samples (in $CDCl_3$) were measured in a 0.1 mm-path length BaF_2 cell with 4 cm^{-1} resolution, 4 h accumulation, and PEM optimized at 1400 cm^{-1}. Spectral baselines were obtained by subtracting the spectra of $CDCl_3$ from the sample spectra. Calculations were carried out with Gaussian03 at DFT level with B3LYP functional/6-31G(d) basis set (center frame) and with B3PW91 functional/TZVP basis set (right frame). Spectra are offset for clarity. Observed VCD spectrum of 4-trifluoromethylphenylglycidol in the 1250–1350 cm^{-1} region are not shown due to artifacts arising from an intense absorbance of C−F stretching at 1325 cm^{-1}.

TABLE 2. Observed versus calculated optical rotations at 589 nm of (*2R*,3*R*)- and (*2S*,3*S*)- enantiomers of 1a through 11b

Enantiomer	Measured OR of (2*R*,3*R*)-:(*2S*,3*S*)- (deg ml/dm g)	Calculated OR[a] of (2*R*,3*R*)- (deg ml/dm g) B3LYP/6-31G(d)	Calculated OR[a] of (2*R*,3*R*)- (deg ml/dm g) B3PW91/TZVP
(*2R*,3*R*)-Phenylglycidol (**1a**):(*2S*,3*S*)-Phenylglycidol (**1b**)	+62:−'62	+115	+83
(*2R*,3*R*)-2-Chlorophenylglycidol (**2a**): (*2S*,3*S*)-2-Chlorophenylglycidol (**2b**)	−6: +7	+108	−7
(*2R*,3*R*)-2-Fluorophenylglycidol (**3a**):(*2S*,3*S*)-2-Fluorophenylglycidol (**3b**)	+44:−38	+16	+29
(*2R*,3*R*)-2-Trifluoromethylphenylglycidol (**4a**):(*2S*,3*S*)-2-Trifluoromethylphenylglycidol (**4b**)	−15: +17	−0.2	−30
(*2R*,3*R*)-3-Chlorophenylglycidol (**5a**): (*2S*,3*S*)-3-Chlorophenylglycidol (**5b**)	+59:−59	+68	+65
(*2R*,3*R*)-3-Fluorophenylglycidol (**6a**): (*2S*,3*S*)-3-Fluorophenylglycidol (**6b**)	+42:−47	+29	+60
(*2R*,3*R*)-3-Methoxyphenylglycidol (**7a**): (*2S*,3*S*)-3-Methoxyphenylglycidol (**7b**)	+56:−44	+46	+77
(*2R*,3*R*)-3-Trifluoromethylphenylglycidol (**8a**): (*2S*,3*S*)-3-Trifluoromethylphenylglycidol (**8b**)	+41:−42	+16	+38
(*2R*,3*R*)-4-Chlorophenylglycidol (**9a**): (*2S*,3*S*)-4-Chlorophenylglycidol (**9b**)	+50:−55	+129	+54
(*2R*,3*R*)-4-Fluorophenylglycidol (**10a**): (*2S*,3*S*)-4-Fluorophenylglycidol (**10b**)	+48:−46	+22	+63
(*2R*,3*R*)-4-Trifluoromethylphenylglycidol (**11a**): (*2S*,3*S*)-4-Trifluoromethylphenylglycidol (**11b**)	+27:−30	+0.2	+36

[a]Calculations carried out with Gaussian 2003.

case of **7a** and **7b**, analytical HPLC employed Chiralpak AD-H and semipreparative SFC employed Chiralpak AS-H. Reversal of elution order is neither uncommon nor predictable,[85–88] and if only UV detection is employed for analysis or enantiomeric preparative separation, without follow-up using measured CD, OR, or VCD, erroneous conclusions can result with respect to correlation of biological activity and (preliminary) assignment of absolute stereochemistry based on HPLC or SFC elution order.

From closer examination of the VCD spectra, four diagnostic absorption bands could be identified that were consistently positive or negative in the respective spectra of all of the enantiomers featuring the same asymmetric configuration in spite of different substituents in the phenyl groups. These vibrational bands represented coupled modes that primarily involve the alcohol and epoxide moieties; however, the phenyl groups are also involved (Fig. 14). Based on Gaussian 2003 analysis, the vibrational

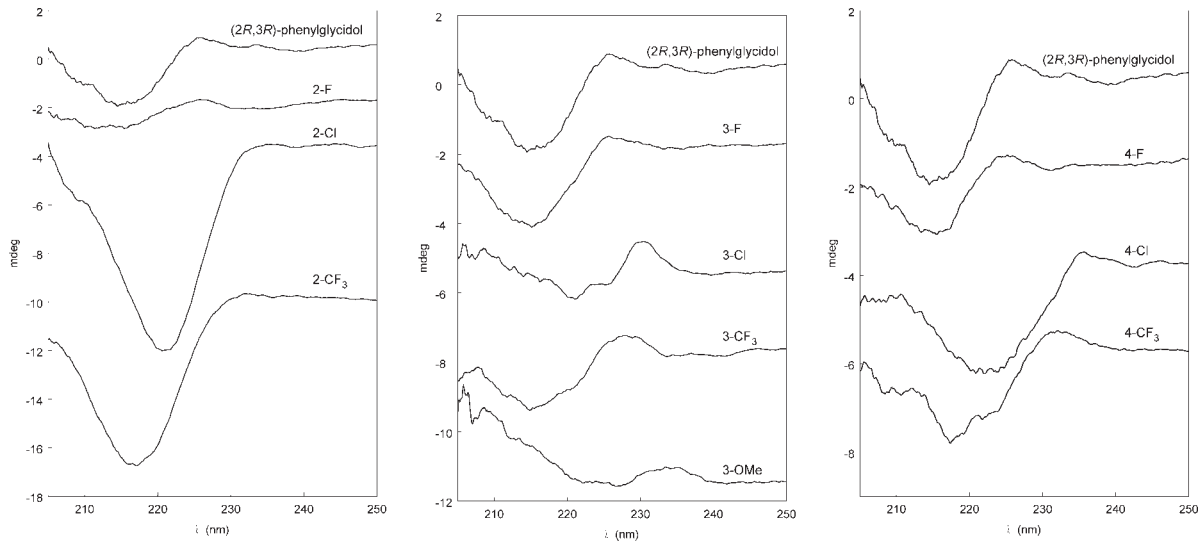

Fig. 13. Observed ECD spectra of the (2*R*,3*R*)-phenylglycidol compounds. Spectra are offset for clarity.

TABLE 3. Observed versus calculated electronic circular dichroism maxima of excited states for the (2*R*,3*R*)-enantiomers of 1a through 11b (see Figure 13 for actual CD spectra)

Enantiomer	Measured ECD excited states – λ_{max} mdeg	Calculated ECD excited states[a] – λ_{max}, rotatory strength (10^{-40} erg esu cm/Gauss)	
		B3LYP/6-31G(d)	B3PW91/TZVP
(2*R*,3*R*)-Phenylglycidol (**1a**)	215, −2; 226, +1	212, +4; 233, +1	214, −3; 234, +1
(2*R*,3*R*)-2-Chlorophenylglycidol (**2a**)	221, −8	213, −5; 222, +5	217, −20; 240, −0.6
(2*R*,3*R*)-2-Fluorophenylglycidol (**3a**)	216, −1; 224, +1	208, −12; 233, −2	213, −2; 236, −3
(2*R*,3*R*)-2-Trifluoromethylphenylglycidol (**4a**)	217, −9	210, −20; 223, +13	212, −11; 239, −4
(2*R*,3*R*)-3-Chlorophenylglycidol (**5a**)	221, −1; 230, +1	214, +0.4; 242, −0.3	218, −1; 242, +1
(2*R*,3*R*)-3-Fluorophenylglycidol (**6a**)	214, −2; 227, +0.3	214, +0.1; 219, −4	214, −2; 237, +0.5
(2*R*,3*R*)-3-Methoxyphenylglycidol (**7a**)	221, −1; 234, +1	214, −14; 224, +3	219, −2.4; 249, +1.7
(2*R*,3*R*)-3-Trifluoromethylphenylglycidol (**8a**)	215, −3; 228, +1	211, −8; 236, +2	218, +1.4; 240, +2.9
(2*R*,3*R*)-4-Chlorophenylglycidol (**9a**)	222, −2; 235, +0.2	212, +2; 223, +13	223, −6; 244, +2
(2*R*,3*R*)-4-Fluorophenylglycidol (**10a**)	215, −2; 225, +0.2	209, −13; 236, +2	213, −5; 240, +4
(2*R*,3*R*)-4-Trifluoromethylphenylglycidol (**11a**)	217, −22; 232, +1	218, −9; 233, +0.2	223, −0.7; 237, +0.06

[a]Calculations carried out with Gaussian 2003.

mode "a" of the lowest-energy conformer of (2*R*,3*R*)-phenylglycidol (**1a**) observed at 1475 cm^{-1} (positive) represents C2—C3 stretching, C2—H and C3—H deformation, phenyl ring C—C stretching, phenyl ring C—H in-plane deformation and C1—H deformation. The vibrational mode "b" observed at 1425 cm^{-1} (negative) represents O—H deformation, C1—H deformation, and C1—C2 stretching. The vibrational mode "c" observed at 1350–1375 cm^{-1} (positive) represents C—H deformations and O—H deformation. The vibrational mode "d" observed at 1075 cm^{-1} (negative) represents C1—O stretching and C—H deformations.

CONCLUSION

Phenylglycidols with a variety of substituents in the phenyl group are prime examples of compounds that can be

TABLE 4. Enantiomeric peak elution (*k*′) from preparative enantiomeric separation by SFC and from analytical HPLC using CSPs

Enantiomer	*K*′ of enantiomer – analytical HPLC[a]	*k*′ of enantiomer – preparative SFC	Preparative CSP, SFC – %MeOH[b]
(2*R*,3*R*)-Phenylglycidol (**1a**)	1.24	NA	NA
(2*S*,3*S*)-Phenylglycidol (**1b**)	1.44	NA	NA
(2*R*,3*R*)-2-Chlorophenylglycidol (**2a**)	1.10	2.93	AD-H-20
(2*S*,3*S*)-2-Chlorophenylglycidol (**2b**)	0.75	1.94	AD-H-20
(2*R*,3*R*)-2-Fluorophenylglycidol (**3a**)	1.22	2.32	AD-H-20
(2*S*,3*S*)-2-Fluorophenylglycidol (**3b**)	0.82	1.47	AD-H-20
(2*R*,3*R*)-2-Trifluoromethylphenylglycidol (**4a**)	0.80[c]	3.03	AD-H-5
(2*S*,3*S*)-2-Trifluoromethylphenylglycidol (**4b**)	0.85[c]	2.72	AD-H-5
(2*R*,3*R*)-3-Chlorophenylglycidol (**5a**)	1.97	4.43	AD-H-25
(2*S*,3*S*)-3-Chlorophenylglycidol (**5b**)	0.78	1.98	AD-H-25
(2*R*,3*R*)-3-Fluorophenylglycidol (**6a**)	2.24	3.25	AD-H-20
(2*S*,3*S*)-3-Fluorophenylglycidol (**6b**)	0.97	1.54	AD-H-20
(2*R*,3*R*)-3-Methoxyphenylglycidol (**7a**)	5.57	1.64	AS-H-10
(2*S*,3*S*)-3-Methoxyphenylglycidol (**7b**)	1.64	1.93	AS-H-10
(2*R*,3*R*)-3-Trifluoromethylphenylglycidol (**8a**)	0.51	1.12	AD-H-15
(2*S*,3*S*)-3-Trifluoromethylphenylglycidol (**8b**)	0.41	0.90	AD-H-15
(2*R*,3*R*)-4-Chlorophenylglycidol (**9a**)	1.03	1.93	AS-H-10
(2*S*,3*S*)- 4-Chlorophenylglycidol (**9b**)	1.29	2.20	AS-H-10
(2*R*,3*R*)-4-Fluorophenylglycidol (**10a**)	0.95	1.86	AS-H-20
(2*S*,3*S*)-4-Fluorophenylglycidol (**10b**)	1.14	2.10	AS-H-20
(2*R*,3*R*)-4-Trifluoromethylphenylglycidol (**11a**)	0.62	2.41	AD-H-10
(2*S*,3*S*)-4-Trifluoromethylphenylglycidol (**11b**)	0.72	2.70	AD-H-10

[a]Analytical HPLC: Chiralpak AD-H (4.6 mm id × 25 cm), 35% EtOH/hexane, 1 ml/min, UV = 225 nm.
[b]Preparative SFC: CSP = Chiralpak AD-H or AS-H (20 mm id × 25 cm, 5 μm) with MeOH in CO_2, 15 ml/min, UV = 220 nm.
[c]Enantiomers co-eluted on Chiralpak AD-H at 35% EtOH/hexane; therefore, *k*′ values recorded using 20% EtOH/hexane.

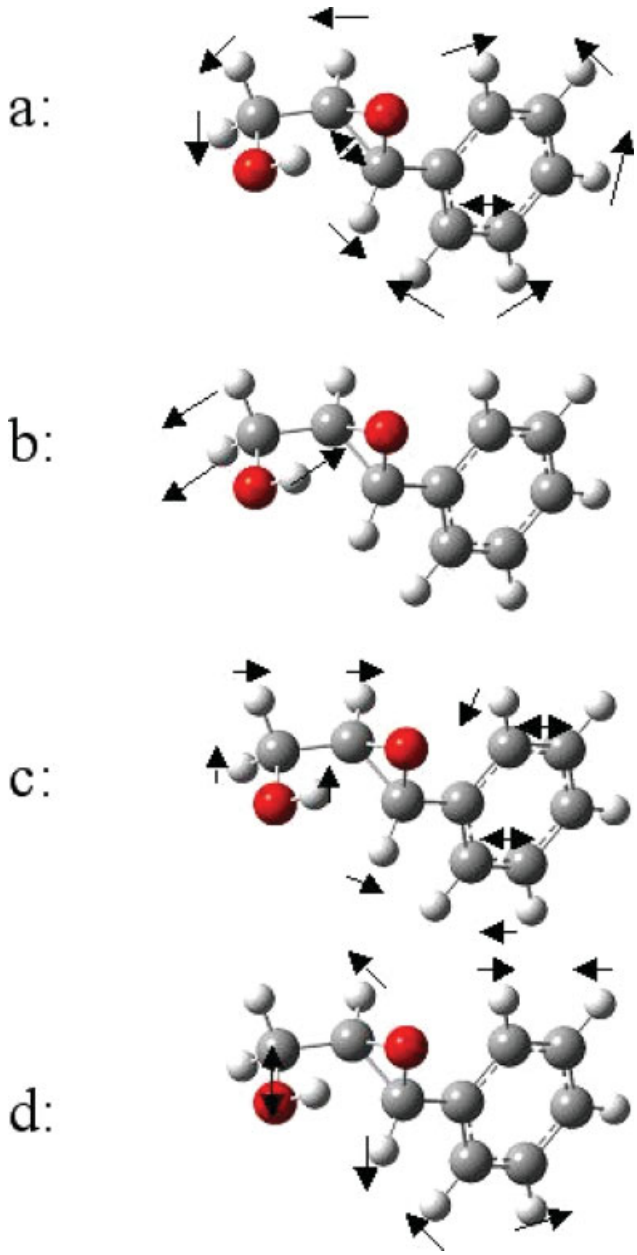

Fig. 14. Vibrational modes of the diagnostic bands a, b, c, and d of the lowest-energy conformer of (2*R*,3*R*)-phenylglycidol(**1a**) (a) C2−C3 stretching, C2−H, and C3−H deformation, phenyl ring C−C stretching, phenyl ring C−H in-plane deformation, and C1−H deformation. (b) O−H deformation, C1−H deformation, and C1−C2 stretching. (c) C−H deformations and O−H deformation. (d) C1−O stretching and C−H deformations.

used in a strategy whereby the absolute stereochemistry of common chiral intermediates is established early in the SAR and SPR phase of a program. That is, phenylglycidols substituted in the phenyl groups with known absolute stereochemistry can readily be elaborated further in one or more steps, perhaps in a parallel synthesis fashion, to yield complex molecules which express a variety of biological properties.

From this study, phenyl substituents in the synthesized molecules were found not to grossly alter spectroscopic features, and therefore, diagnostic absorption bands in the respective VCD spectra, the sign and shape of observed ECD curves, and could be used to determine and track the absolute stereochemistry of analogs without necessarily requiring time-consuming ab initio calculations of all low energy conformers for all compounds. In this series, comparison of calculated and measured VCD, OR, and ECD was especially useful when using the hybrid B3PW91 functional and the TZVP basis set; in all cases, either calculated VCD, OR, or ECD could have been used to accurately assign absolute stereochemistry. However, when using the B3LYP functional with the 6-31G(d) basis set, calculated VCD could be used to accurately assign absolute stereochemistry, but calculated ECD spectra and some of the calculated OR values did not compare favorably with observed spectra and values, respectively.

ACKNOWLEDGMENTS

We thank Callain Kim for her interest in substituted, enantiomeric phenylglycidols that helped stimulate the study described above, acknowledge the ongoing support of Wyeth management in Chemical and Screening Sciences, in particular, Dr. G. Carter and Dr. M. Abou-Gharbia, and acknowledge the support, input, and feedback of our colleagues (Dr. R. Dukor (BioTools, Inc), Prof. L. Nafie (Syracuse University), Prof. N. Berova (Columbia University), Prof. P. Polavarapu (Vanderbilt University), Dr. T. Berger (AccelaPure), and Dr. Y. Zhang (BMS)).

LITERATURE CITED

1. Marino S, Starchursk-Buczek D, Huggins D, Krywult B, Sheehan C, Nguyen T, Choi N, Parsons J, Griffiths P, James I, Bray AM, White JM, Boyce RS. Synthesis of chiral building blocks for use in drug discovery. Molecules 2004;9:405–426.
2. Beck G. Synthesis of chiral drug substances. Synlett 2002:837–850.
3. Loiseleur O, Koch G, Wagner T. A practical building block for the synthesis of discodermolide. Org Process Res Dev 2004;8:597–602.
4. Patel R, Goswami A, Chu L, Donovan M, Nanduri V, Goldberg S, Johnston R, Siva P, Nielsen B, Fan J and others. Enantioselective microbial reduction of substituted acetophenones. Tetrahedron: Asymmetry 2004; 15:1247–1258.
5. Arisawa A, Matsufuji M, Nakashima T, Dobashi K, Isshiki K, Yoshioka T, Yamada S, Momose H, Taguchi S. Streptomyces serine protease (DHP-A) as a new biocatalyst capable of forming chiral intermediates of 1,4-dihydropyridine calcium antagonists. App Environ Microbiol 2002;68:2716–2725.
6. Zong-De Z, Yan-Ping S, Ting W. Development and validation of HPLC methods for enantioseparation of mirtazapine enantiomers at analytical and semipreparative scale using polysaccharide chiral stationary phases. Anal Chim Acta 2005;550:123–129.
7. Andersson S, Allenmar S. Preparative chiral chromatographic resolution of enantiomers in drug discovery. J Biochem Biophys Methods 2002;54:11–23.
8. Francotte E. Enantioselective chromatography as a powerful alternative for the preparation of drug enantiomers. J Chromatogr A 2001;906: 379–397.
9. Kennedy J, Bowers J, Dodge J, Lugar C, Shepherd T, Sharp V. Development of analytical and preparative chromatographic separations of novel growth hormone secretagogue compounds. J Chromatogr A 2000; 872:75–84.
10. Kellogg R, Nieuwenhuijzen J, Pouwer K, Vries T, Broxterman Q, Grimbergen R, Kaptein B, Crois FL, Wever ED, Zwaagstra K and others. Dutch resolution: Separation of enantiomers with families of resolving agents. A status report. Synthesis 2003;10:1626–1638.

11. Kaptein B, Vries T, Nieuwenhuijzen J, Kellogg R, Grimbergen R, Broxterman Q. Continuous developments in classical resolution: Dutch resolution and asymmetric transformation. Life Sci Adv Syn Catal Pharmachem 2003;2:17–22.
12. Martinez A, Alonso M, Castro A, Dorronsoro I, Gelpi J, Luque F, Perez C, Moreno F. SAR and 3D-QSAR studies on thiadiazolidinone derivatives: Exploration of structural requirements for glycogen synthase kinase 3 inhibitors. J Med Chem 2005;48:7103–7112.
13. Chesworth R, Wessel M, Heyden L, Mangano F, Zawistoski M, Gegnas L, Galluzzo D, Lefker B, Cameron K, Tickner J, Lu B, Castleberry, Petersen DN, Brault A, Perry P, Ng O, Owen TA, Pan L, Ke H-Z, Brown TA, Thompson DD, DeSilva-Jardine P. Estrogen receptor β selective ligands: Discovery and SAR of novel heterocyclic ligands. Bioorg Med Chem Lett 2005;15:5562–5566.
14. Kling A, Lange W, Mack H, Bakker M, Drescher K, Hornberger W, Hutchins C, Moller A, Muller R, Schmidt M, Unger L, Wicke K, Schellhaas K, Steiner. Synthesis and SAR of highly potent dual 5-HT1A and 5-HT1B antagonists as potential antidepressant drugs. Bioorg Med Chem Lett 2005;15:5567–5573.
15. Nassar A-E, Kamel A, Clarimont C. Improving the decision-making process in the structural modification of drug candidates. Drug Discov Today 2004;9:1020–1028.
16. Fichert T, Yazdanian M, Proudfoot J. A structure-permeability study of small drug-like molecules. Bioorg Med Chem Lett 2003;13:719–722.
17. Veber D, Johnson S, Cheng H-Y, Smith B, Ward K, Kopple K. Molecular properties that influence the oral bioavailability of drug candidates. J Med Chem 2002;45:2615–2623.
18. Goodwin J, Conradi R, Ho N, Burton P. Physicochemical determinants of passive membrane permeability: Role of solute hydrogen-bonding potential and volume. J Med Chem 2001;44:3721–2729.
19. van de Waterbeemd H, Smith D, Beaumont K, Walker D. Property-based design: Optimization of drug absorption and pharmacokinetics. J Med Chem 2001;44:1313–1333.
20. Di L, Kerns E. Application of pharmaceutical profiling assays for optimization of drug-like properties. Curr Opin Drug Discov Dev 2005;8: 495–504.
21. Chimenti F, Maccioni E, Secci D, Bolasco A, Chimenti P, Granese A, Befani O, Turini P, Alcaro S, Ortuso F, Cirilla, La Torre F, Cardia MC, Distinto S. Synthesis, molecular modeling studies, and selective inhibitory activity against monoamine oxidase of 1-thiocarbamoyl-3,5-diaryl-4,5 dihydro-(qH)-pyrazole derivatives. J Med Chem 2005;48:7113–7122.
22. Chu-Moyer M, Ballinger W, Beebe D, Coutcher J, Day W, Li J, Oates P, Weekly R. SAR and species/stereoselective metabolism of the sorbitol dehydrogenase inhibitor, CP-470,711. Bioorg Med Chem Lett 2002;12:1477–1480.
23. Zhang Y, Wu D-R, Want-Iverson D, Tymiak A. Enantioselective chromatography in drug discovery. Drug Discov Today 2005;8:571–577.
24. Liu Y, Lantz A, Armstrong D. High efficiency liquid and super-subcritical fluid-based enantiomeric separations: An overview. J Liquid Chromatogr Relat Technol 2004:27:1121–1178.
25. Welch C, Jr WL, DaSilva J, Biba M, Albaneze-Walker J, Henderson D, Laing B, Mathre D. Preparative chiral SFC as a green technology for rapid access to enantiopurity in pharmaceutical process research. LC-GC 2005;23:16–29.
26. Maas G. Determination of absolute and relative configuration by X-ray and neutron diffraction methods. In: Houben-Weyl, editor. Methoden der Organischen Chemie, Band E21/1. Stuttgart: Thieme Verlag; 1995.
27. Stout G, Jensen L. X-ray structure determination: A practical guide, 2nd ed. New York: Wiley; 1989. 480 p.
28. Devlin F, Stephens P, Besse P. Are the absolute configurations of 2-(1-hydroxyethyl)-chromen-4-one and its 6-bromo derivative determined by X-ray crystallography correct? A vibrational circular dichroism study of their acetate derivatives. Tetrahedron: Asymmetry 2005;16: 1557–1566.
29. Li J, Burgett A, Amezcua C, Harran P. Total synthesis of nominal diazonamides—Part 2: On the true structure and origin of the natural isolates. Angew Chem Int Ed Engl 2001;40:4770–4773.
30. Seco J, Quinoa E, Riguera R. The assignment of absolute configuration by NMR. Chem Rev 2004;104:17–117.
31. Seco J, Quinoa E, Riguera R. A practical guide for the assignment of the abolsute configuration of alcohols, amines and carboxylic acids by NMR. Tetrahedron: Asymmetry 2001;12:2915–2925.
32. Schlingmann G, Roll D. Absolute stereochemistry of unusual biopolymers from Ascomycete culture LL-W1278: Examples that derivatives of (*S*)-6-hydroxymellein are also natural fungal metabolites. Chirality 2005;17:S48–S51.
33. Bari LD, Mannuccci S, Pescitelli G, Salvadori P. Assignment of absolute configuration of chiral carboxylic acids via exciton-coupled CD treatment: 4-Phenylthioproline as a case study. Chirality 2002;14:611–617.
34. Meguro H, Kim J-H, Bai C, Nishida Y, Ohrui H. Some applications of a chiral fluorometric reagent, (*S*)-TBMB carboxylic acid. Chirality 2001;13:441–445.
35. Spodine E, Zolezi S, Calvo V, Decinti A. Studies of the circular dichroism spectra of dissymmetric Schiff-bases by means of the exciton chirality method. Tetrahedron: Asymmetry 2000;11:2277–2288.
36. Hartl M, Humpf H-U. 2-Naphthol as a powerful chromophore for the configurational assignment of carboxylic acid groups via the CD exciton chirality method. Tetrahedron: Asymmetry 2000;11:1741–1747.
37. Huang X, Fujioka N, Pescitelli G, Koehn F, Williamson R, Nakanishi K, Berova N. Absolute configurational assignments of secondary amines by CD-sensitive dimeric zinc porphyrin host. J Am Chem Soc 2002;124:10320–10335.
38. Kurtan T, Nesnas N, Li Y-Q, Huang X, Nakanishi K, Berova N. Chiral recognition by CD-sensitive dimeric zinc porphyrin host, Part 1: Chiroptical protocol for absolute configurational assignments of monoalcohols and primary monamines. J Am Chem Soc 2001;123:5962–5973.
39. Kurtan T, Nesnas N, Koehn F, Li Y-Q, Nakanishi K, Berova N. Chiral recognition by CD-sensitive dimeric zinc porphyrin host, Part 2: Structural studies of host-guest complexes with chiral alcohol and monamine conjugates. J Am Chem Soc 2001;123:5974–5982.
40. Freedman T, Cao X, Dukor R, Nafie L. Absolute configuration determination of chiral molecules in the solution state using vibrational circular dichroism. Chirality 2003;15:743–758.
41. Stephens P. Vibrational circular dichroism spectroscopy: A new tool for the stereochemical characterization of chiral molecules. Comput Med Chem Drug Discov 2004:699–725.
42. Polavarapu P. Optical rotation: Recent advances in determining the absolute configuration. Chirality 2002;14:768–781.
43. Polavarapu P, Petrovic A, Wang F. Intrinsic rotation and molecular structure. Chirality 2003;15(Suppl):S143–S149.
44. Stephens P, Devlin F, Cheeseman J, Frisch M, Bortoline O, Besse P. Determination of absolute configuration using ab initio calculation of optical rotation. Chirality 2003;15(Suppl):S57–S64.
45. Superchi S, Giogio E, Rosini C. Structural determinations by circular dichroism spectra analysis using coupled oscillator methods: An update of the applications of the DeVoe polarizability model. Chirality 2004;16:422–451.
46. Stephens P, McCann D, Butkus E, Stoncius S, Cheeseman J, Frisch M. Determination of absolute configuration using concerted ab initio DFT calculations of electronic circular dichroism and optical rotation: bicyclo[3.3.1]nonane diones. J Org Chem 2004;69:1948–1958.
47. Stephens P, McCann D, Devlin F, Cheeseman J, Frisch M. Determination of the absolute configuration of [3.2](1,4)barrelenophanedicarbonnitrile using concerted time-dependent density functional theory calculations of optical rotation and electronic circular dichroism. J Am Chem Soc 2004;126:7514–7521.
48. Petrovic A, He J, Polavarapu P, Xiao L, Armstrong D. Absolute configuration and predominant conformations of 1,1-dimethyl-2-phenylethyl phenyl sulfoxide. Org Biomol Chem 2005;3:1977–1981.
49. Petrovic A, Polavarapu P, Drabowicz J, Zhang Y, McConnell O, Duddeck H. Absolute configuration of C2-symmetric spiroselenurane: 3,3,3′3′-Tetramethyl-1,1′spriobi[3H. 2.1]benzoxaselenole. Chem—Eur J 2005;11:4257–4262.
50. Freedman T, Cao X, Nafie L, Kalbermatter M, Linden A, Rippert A. Determination of the atropisomeric stability and solution conformation of asymmetrically substituted biphenyls by means of vibrational circular dichroism (VCD). Helv Chim Acta 2005;88:2302–2314.

51. Cichewicz R, Clifford L, Lassen P, Freedman XCT, Nafie L, Deschamps J, Kenyon V, Flanary J, Holman T, Crews P. Stereochemical determination and bioactivity assessment of (S)-(+)-curcuphenol dimers isolated from the marine sponge *Didiscus aceratus* and synthesized through laccase biocatalysis. Bioorg Med Chem 2005;13:5600–5612.
52. Freedman T, Cao X, Oliveira R, Cass Q, Nafie L. Determination of the absolute configuration and solution conformation of gossypol by vibrational circular dichroism. Chirality 2003;15:196–200.
53. Freedman T, Nafie XCL, Kalbermatter M, Linden A, Rippert A. An unexpected atropisomerically stable 1,1-biphenyl at ambient temperature in solution, elucidated by vibrational circular dichroism (VCD). Helv Chim Acta 2003;86:3141–3155.
54. Dunmire D, Freedman T, Nafie L, Aeschlimann C, Gerber J, Gal J. Determination of the absolute configuration and solution conformation of the antifungal agents ketoconazole, itraconazole, and miconazole with vibrational circular dichroism. Chirality 2005;17:S101–S108.
55. Freedman T, Cao X, Nafie L, Solladie-Cavallo A, Jierry I, Bouerat L. VCD configuration of enantiopure-enriched tetrasubstituted α-fluorocyclohexanones and their use for epoxidation of *trans*-olefins. Appl Spectrosc 2004;59:1114–1124.
56. Guo C, Shah R, Dukor R, Cao X, Freedman T, Nafie L. Determination of enantiomeric excess in samples of chiral molecules using Fourier transform vibrational circular dichroism spectroscopy: Simulation of real-time reaction monitoring. Anal Chem 2004;76:6956–6966.
57. Maryanoff B, McComsey D, Dukor R, Nafie L, Freedman T, Cao X, Day V. Structural studies on McN-5652-X, a high-affinity ligand for the serotonin transporter in mammalian brain. Bioorg Med Chem 2003;11:2463–2470.
58. Freedman T, Dukor R, Hoof PV, Bach EK, Nafie L. Determination of the absolute configuration of (−)-mirtazapine by vibrational circular dichroim. Helv Chim Acta 2002;85:1160–1165.
59. Shah R, Nafie L. Spectroscopic methods for determining enantiomeric purity and absolute confguration in chiral pharmaceutical molecules. Curr Opin Drug Discov Dev 2001;4:764–775.
60. Solladie-Cavallo A, Marsol C, Pescitelli G, DiBari L, Salvadori P, Huang X, Fujioka N, Berova N, Cao X, Freedman T and others. (*R*)-(+)- and (*S*)-(−)-1-(9-phenanthryl)ethylamine: Assignment of absolute configuration by CD tweezer and VCD methods, and difficulties encountered with the CD exciton chirality method. Eur J Org Chem 2002;11:1788–1796.
61. Stephens P, McCann D, Cheeseman J, Frisch F. Determination of absolute configurations of chiral molecules using ab inito time-dependent density functional theory calculations of optical rotation: How reliable are absolute configurations obtained for molecules with small rotations? Chirality 2005;17:S52–S64.
62. Goument B, Duhamel L, Mauge R. Asymmetric syntheses of (*S*)-fenfluramine using sharpless epoxidation methods. Tetrahedron 1994;50:171–188.
63. Gao Y, Sharpless K. Asymmetric synthesis of both enantiomers of tomoxetine and fluoxetine. Selective reduction of 2,3-epoxycinnamylalcohol with Red-Al. J Org Chem 1988;53:4081–4084.
64. Denis J-N, Greene A, Serra A, Luche M-J. An efficient, enantioselective synthesis of the taxol side chain. J Org Chem 1986;51:46–50.
65. Wroblewski A, Piotrowska D. Enantiomeric phosphonate analogs of the paclitaxel C-13 side chain. Tetrahedron: Asymmetry 1999;10:2037–2043.
66. Testa M, Hajji C, Zaballos-Garcia E, Garcia-Sergovia A, Sepulveda-Arques J. Asymmetric synthesis of (−)-pseudoephedrine from (2*S*,3*S*)-3-phenyloxiran-2-ylmethanol. Stereospecific interchange of amino and alcohol functions. Tetrahedron: Asymmetry 2001;12:1369–1372.
67. Chen J, Lin G-Q, Liu H-Q. Stereoselective synthesis of the styryllactones, 7-epi-goniodiol and leiocarpin A, isolated from *Gonionthalamus leiocarpus*. Tetrahedron Lett 2004;45:8111–8113.
68. Yang Z-C, Zhou W-S. Asymmetric total synthesis of (+)-goniotriol and (+)-goniofulurone. Tetrahedron 1995;51:1429–1436.
69. Yadav J, Rajaiah G, Raju A. A concise and stereoselective synthesis of both enantiomers of altholactone and isoaltholactone. Tetrahedron Lett 2003;44:5831–5833.
70. Chen X, Gu W, Jing X, Pan X. A new approach for synthesis of *erythro* 8-*O*-4′ neolignans. Synth Commun 2002;32:557–564.
71. Bartoli G, Bosco M, Carolone A, Locatelli M, Masaccesi, Melchiorre P, Sambri L. Asymmetric aminolysis of aromatic epoxides: A facile catalytic enantioselective synthesis of anti-β-amino alcohols. Org Lett 2004;6:2173–2176.
72. Schomaker J, Pulgam V, Borhan B. Synthesis of diastereomerically and enantiomerically pure 2,3-disubstituted tetrahydrofurans using a sulfoxonium ylide. J Am Chem Soc 2004;126:13600–13601.
73. Islas-Gonzalez G, Puigjaner C, Vidal-Ferran A, Moyano A, Riera A, Pericas M. Boron trifluoride-induces reactions of phenylglycidyl ethers: A convenient synthesis of enantiopure, stereodefined fluorohydrins. Tetrahedron Lett 2004;45:6337–6341.
74. Melloni P, DellaTorre A, Lazzari E, Mazzini G, Meroni M. Configurational studies on 2-[α-(2-ethoxyphenoxy)benzyl] morpholine fce 20124. Tetrahedron 1985;41:1393–1399.
75. Konno H, Toshiro E, Hinoda N. An epoxide ring-opening reaction via hypervalent silicate intermediate: Synthesis of statine. Synthesis 2003;14:2161–2164.
76. Powell J, Johnson EM II, Gannett P. Improvement of a critical intermediate step in the synthesis of a nitroxide-based spin-labeled deoxythymidine analog. Molecules 2000;5:1244–1250.
77. Srinivasan R, Chandrasekharam M, Vani P, Chida A, Singh A. Epoxidation of olefins at low temperature using *m*-chloroperbenzoic acid. Synth Commun 2002;32:1853–1858.
78. von Sprecher A, Beck A.Preparation of 7-(1-hydroxy-ω-phenoxyalken-2-ylthio)benzophyran-4-one-carboxylates and anlogs as leukotriene and phospholipase inhibitors. Germany Patent 19890328; 1989.
79. Boulet S, Filla S, Gallagher P, Hudziak K, Johannson A, Karanjawala R, Masters J, Matassa V, Mathes B, Rathmell R and others. Preparation of 3-aryloxy/thio-2, 3-substituted propanamines and their use in inhibiting serotonin and norepinephrine reuptake. Patent 200310024; 2004.
80. Evans D, Gauchet-Prunet J, Carreira E, Charette A. Synthesis of 1,3-diol synthons from epoxy aromatic precursors: An approach to the construction of polyacetate-derived natural products. J Org Chem 1991;56:741–750.
81. Goument B, Duhamel L, Mauge R. Epoxides, amino alcohols and axiridines as key intermediates in the asymmetric synthesis of (*S*)-fenfluramine. Bull Soc Chim Fr 1993;130:459–466.
82. Shi L, Want W, Huang Y-Z. A novel synthesis of 2,3-epoxy-3-arylpropanol via arsonium salt. Tetrahedron Lett 1988;29:5295–5296.
83. Perez SM-ZY, delHierro I, Fajardo M, Sierra I. Simultaneous determination of phenylglycidol enantiomers and cinnamyl alcohol in asymmetric epoxidation processes by chiral liquid chromatography. J Chromatogr A 2004;1046:61–66.
84. Devlin F, Stephens P, Bortolini O. Determination of absolute configuration using vibrational circular dichroism spectroscopy: Phenyl glycidic acid derivatives obtained via asymmetric epoxidation using oxone and a keto bile acid. Tetrahedron: Asymmetry 2005;16:2653–2663.
85. Gyllenhaal O, Stefansson M. Reversal of elution order for profen acid enantiomers in packed-column SFC on Chiralpak AD. J Chirality 2005;17:257–265.
86. Okamoto M. Reversal of elution order during the chiral separation in high performance liquid chromatography. J Pharm Biomed Anal 2002;27:401–407.
87. Xiao T, Zhang B, Lee J, Hui F, Armstrong D. Reversal of enantiomeric elution order on macrocyclic glycopeptide chiral stationary phases. J Liq Chromatogr Relat Technol 2001;24:2673–2684.
88. Roussel C, Vanthuyne N, Serradeil-Albalat M, Vallejos J-C. True or apparent reversal of elution order during chiral high-performance liquid chromatography monitored by a polarimetric detector under different mobile phase conditions. J Chromatogr A 2003;995:79–85.